

K. Osada, Y. Yamasaki, S. Katayose, K. Kataoka	A synthetic block copolymer regulates SI nuclease fragmentation of super-coiled plasmid DNA	Angew. Chem., Int'l. Ed	in press		2005
M. Oishi, S. Sasaki, Y. Nagasaki, K. Kataoka	Smart polyion complex micelles for targeted intracellular delivery of PEGylated antisense oligonucleotide with acid-labile linkage	ChemBioChem	in press		2005
K. Uchida, H. Otsuka, M. Kaneko, K. Kataoka, Y. Nagasaki	A reactive poly(ethylene glycol) layer to achieve specific surface plasmon resonance sensing with a high S/N ratio: the substantial role of a short underbrushed PEG layer in minimizing nonspecific adsorption	Anal. Chem.	77 (4)	1075-1080	2005
S. Fukushima, K. Miyata, N. Nishiyama, N. Kanayama, Y. Yamasaki, K. Kataoka	PEGylated polyplex micelles from triblock cationomers with spatially-ordered layering of condensed pDNA and buffering units for enhanced intracellular gene delivery	J. Am. Chem. Soc	127 (9)	2810-2811	2005
M. Oishi, Y. Nagasaki, K. Itaka, N. Nishiyama, K. Kataoka	Lactosylated Poly(ethylene glycol)-siRNA conjugate through acid-labile β -thiopropionate linkage to construct pH-sensitive polyion complex micelles achieving enhanced gene silencing in hepatoma cells	J. Am. Chem. Soc	127 (6)	1624-1625	2005
W.-D. Jang, N. Nishiyama, G.-D. Zhang, A. Harada, D.-L. Jiang, S., Y. Morimoto, M. Kikuchi, H. Koyama, T. Aida, K. Kataoka	Supramolecular nanocarrier of anionic dendrimer porphyrins with PEGylated cationic block co-polymer to enhance intracellular photodynamic efficacy	Angew. Chem., Int'l. Ed	44 (3)	419-423	2005
K. Itaka, N. Kanayama, N. Nishiyama, Y. Yamasaki, K.	Supramolecular nano-carrier of siRNA from PEG-based block cationomer carrying diamine side-chain with distinctive	J. Am. Chem. Soc.	126 (42)	13612-13613	2004

Nakamura, H. Kawaguchi, K. Kataoka	pKa directed to enhance intracellular gene silencing				
Y. Kakizawa, K. Miyata, S. Furukawa, K. Kataoka	Size-controlled formation of a calcium phosphate-based organic-inorganic hybrid vector for gene delivery using poly(ethylene glycol)-block-poly(aspartic acid),	Advanced Materials	16 (8)	699-702	2004
K. Miyata, Y. Kakizawa, N. Nishiyama, A. Harada, Y. Yamasaki, H. Koyama, K. Kataoka	Block cationic polyplexes with regulated densities of charge and disulfide cross-linking directed to enhance gene expression	J. Amer. Chem. Soc.	126 (8)	2355-2361	2004
M. Tabuchi, M. Ueda, N. Kaji, Y. Yamasaki, Y. Nagasaki, K. Yoshikawa, K. Kataoka, Y. Baba,	Nano-spheres for DNA separation chips	Nature Biotechnology	22 (3)	337-340	2004
R. Ideta, Y. Yanagi, Y. Tamaki, F. Tasaka, A. Harada, K. Kataoka	Effective accumulation of polyion complex micelle to experimental choroidal neovascularization in rats	FEBS Lett	557 (1-3)	21-25	2004
K. Itaka, A. Harada, Y. Yamasaki, K. Nakamura, H. Kawaguchi, K. Kataoka	In situ single cell observation by fluorescence resonance energy transfer reveals fast intra-cytoplasmic delivery and easy release of plasmid DNA complexed with linear poly-ethylenimine	J. Gene Med.	6 (1)	76-84	2004
K. Nishida, M. Yamato, Y. Hayashida, K. Watanabe, K. Yamamoto, E. Adachi, S. Nagai, A. Kikuchi, N.	Corneal reconstruction with tissue-engineered cell sheets composed of autologous oral mucosal epithelium	N. Engl. J. Med.	351 (12)	1187-1196	2004

Maeda, H. Watanabe, T. Okano and Y. Tano					
M. Yamato and T. Okano	Cell Sheet Engineering	Materialstoday	May 2004	42-47	2004
J. Yang, M. Yamato, T. Okano	Cell-Sheet Engineering Using Intelligent Surfaces	MRS Bulletin	30	189-193	2005

The Combination of SOX5, SOX6, and SOX9 (the SOX Trio) Provides Signals Sufficient for Induction of Permanent Cartilage

Toshiyuki Ikeda,¹ Satoru Kamekura,² Akihiko Mabuchi,¹ Ikuyo Kou,¹ Shoji Seki,¹ Tsuyoshi Takato,³ Kozo Nakamura,² Hiroshi Kawaguchi,² Shiro Ikegawa,¹ and Ung-il Chung³

Objective. To regenerate permanent cartilage, it is crucial to know not only the necessary conditions for chondrogenesis, but also the sufficient conditions. The objective of this study was to determine the signal sufficient for chondrogenesis.

Methods. Embryonic stem cells that had been engineered to fluoresce upon chondrocyte differentiation were treated with combinations of factors necessary for chondrogenesis, and chondrocyte differentiation was detected as fluorescence. We screened for the combination that could induce fluorescence within 3 days. Then, primary mesenchymal stem cells, nonchondrogenic immortalized cell lines, and primary dermal fibroblasts were treated with the combination, and the induction of chondrocyte differentiation was assessed by detecting the expression of the cartilage marker genes and the accumulation of proteoglycan-rich matrix. The effects of monolayer, spheroid, and 3-dimensional culture systems on induction by combinations of transcription

factors were compared. The effects of the combination on hypertrophic and osteoblastic differentiation were evaluated by detecting the expression of the characteristic marker genes.

Results. No single factor induced fluorescence. Among various combinations examined, only the SOX5, SOX6, and SOX9 combination (the SOX trio) induced fluorescence within 3 days. The SOX trio successfully induced chondrocyte differentiation in all cell types tested, including nonchondrogenic types, and the induction occurred regardless of the culture system used. Contrary to the conventional chondrogenic techniques, the SOX trio suppressed hypertrophic and osteogenic differentiation at the same time.

Conclusion. These data strongly suggest that the SOX trio provides signals sufficient for the induction of permanent cartilage.

Utilizing the differentiation and proliferation capabilities of stem cells, regenerative medicine attempts to treat irreversible organ failures that cannot be dealt with by conventional medical treatment. In the skeletal area, cartilage has a relatively poor regenerative capacity and, thus, may benefit most from regenerative medicine. Conditions such as osteoarthritis and congenital skeletal defects are apparent targets that have great medical and socioeconomic impact. To make cartilage regenerative medicine a reality, it is essential to know the conditions that are both necessary and sufficient for chondrogenesis.

A number of factors have been shown to be vital for chondrogenesis. These factors include the sex-determining region Y-type high mobility group box (SOX) family of transcription factors (1), insulin-like growth factor 1 (IGF-1) (2), fibroblast growth factor 2 (FGF-2) (3), Indian hedgehog (IHH) (4), bone morpho-

Dr. Ikegawa's work was supported by a grant from the Japanese Millennium Project and a Grant-in-Aid for Scientific Research from the Japanese Ministry of Education, Culture, Sports, Science, and Technology (14207055). Dr. Chung's work was supported by a Grant-in-Aid for Scientific Research from the Japanese Ministry of Education, Culture, Sports, Science, and Technology (15390452) and by a generous endowment from Takeda Chemical Industries, Osaka, Japan.

¹Toshiyuki Ikeda, MD, Akihiko Mabuchi, MD, Ikuyo Kou, MEng, Shoji Seki, MD, Shiro Ikegawa, MD, PhD: SNP Research Center, RIKEN (The Institute of Physical and Chemical Research), Tokyo, Japan; ²Satoru Kamekura, MD, Kozo Nakamura, MD, PhD, Hiroshi Kawaguchi, MD, PhD: University of Tokyo Graduate School of Medicine, Tokyo, Japan; ³Tsuyoshi Takato, MD, PhD, Ung-il Chung, MD, PhD: University of Tokyo Hospital, Tokyo, Japan.

Address correspondence and reprint requests to Shiro Ikegawa, MD, PhD: Laboratory for Bone and Joint Diseases, SNP Research Center, RIKEN, c/o Institute of Medical Science, University of Tokyo, 4-6-1 Shirokanedai, Minato-ku, Tokyo 108-8639, Japan. E-mail: sikegawa@ims.u-tokyo.ac.jp.

Submitted for publication February 25, 2004; accepted in revised form August 2, 2004.

genetic protein 2 (BMP-2) (5), transforming growth factor β (TGF β) (6), and Wnt proteins (4).

Many lines of evidence, both in vitro and in vivo, have shown that SOX proteins are necessary for chondrogenesis. SOX9 is expressed in all chondroprogenitors and chondrocytes except hypertrophic chondrocytes (7,8). Heterozygous mutations of *SOX9* cause a severe chondrodysplasia, known as campomelic dysplasia, in humans (9,10). Analysis of chimeric mice containing wild-type and *Sox9*-deficient cells showed that the mutant cells were excluded from chondrogenic mesenchymal condensation and failed to express chondrocyte-specific marker genes (11). SOX9 was shown to bind to and activate chondrocyte-specific enhancer elements in *Col2a1*, *Col9a1*, *Col11a2*, and *Aggrecan* in vitro (12–18). Conditional ablation of the *Sox9* gene in limb buds before mesenchymal condensation resulted in a complete absence of chondrocytes, whereas conditional ablation of *Sox9* after mesenchymal condensation resulted in a severe generalized chondrodysplasia (19). Two other members of the Sox family, *Sox5* and *Sox6*, are also required for chondrogenesis. *Sox5*^{-/-} and *Sox6*^{-/-} mice show chondrodysplastic phenotypes and die at birth. *Sox5*^{-/-} and *Sox6*^{-/-} mice develop a severe, generalized chondrodysplasia characterized by a virtual absence of cartilage (20). In vitro studies have shown that *Sox5* and *Sox6* cooperate with *Sox9* to activate the *Col2a1* enhancer in chondrogenic cells (21).

Although these lines of evidence demonstrate that these factors are necessary for chondrogenesis, no single factor has proved sufficient for the process. That is, we do not yet know what constitutes a sufficient signal for chondrogenesis. In the current study, we sought to determine the sufficient signal by screening various combinations of known factors that are necessary for chondrogenesis.

MATERIALS AND METHODS

Construction of plasmid vectors and adenoviruses.

Combinations of known factors important for chondrogenesis were screened. These factors included SOX5, SOX6, SOX9, IGF-1, FGF-2, IHH, BMP-2, TGF β , and Wnt proteins. For each signaling pathway, we constructed an adenovirus vector that stimulates the pathway (overexpression of the wild-type form or expression of the constitutively active form) as well as one that inhibits the pathway (expression of the dominant-negative form or RNA interference [RNAi] form).

We then stimulated the signaling and inhibition of each factor. SOX signaling was stimulated as described below. To stimulate SOX inhibition, we constructed adenoviruses expressing RNAi for SOX5, SOX6, and SOX9 (22). To stimulate IGF-1 signaling, we used an adenovirus expressing

insulin receptor substrate 1 (IRS-1); to inhibit, we used one expressing a dominant-negative form of IRS-1 (23). To stimulate FGF signaling, we constructed an adenovirus expressing a constitutively active form of FGF receptor 3 (FGFR-3); to inhibit, we used one expressing RNAi for FGFR-3 (24). To stimulate IHH signaling, we constructed an adenovirus expressing constitutively active Smoothed (25); to inhibit, we used one expressing a repressor form of Gli-3 (26). To stimulate BMP signaling, we used an adenovirus expressing a constitutively active form of activin receptor-like kinase 6 (ALK-6); to inhibit, we used one expressing Smad6 (27). To stimulate TGF β signaling, we used an adenovirus expressing a constitutively active form of ALK-5; to inhibit, we used one expressing Smad7 (27). To stimulate Wnt signaling, we constructed an adenovirus expressing a constitutively active form of T cell factor (TCF); to inhibit, we used one expressing a dominant-negative form of TCF (28).

As a control vector, we used the adenovirus expressing the β -galactosidase gene *lacZ*. Thus, for each signaling pathway, there were 3 adenoviruses (positive, negative, and neutral). To create combinations, one adenovirus from each signaling pathway was selected and mixed with another.

To create adenoviruses expressing SOX5, SOX6, and SOX9, full-length human *SOX5*, *SOX6*, and *SOX9* complementary DNA (cDNA) was amplified by polymerase chain reaction (PCR) and cloned into pEGFP1 and pShuttle mammalian expression vectors (Clontech, Palo Alto, CA). We confirmed that the introduced green fluorescence protein (GFP) tags did not interfere with the activities of any SOX. PCR products were verified by DNA sequencing. Adenovirus vectors expressing SOX5, SOX6, and SOX9 were constructed with the AdenoX Expression system (Clontech), according to the manufacturer's instructions. Adenovirus vector expressing LacZ was provided by the manufacturer. Adenoviruses were packaged and amplified in HEK 293 cells and purified with an AdenoX virus purification kit (Clontech). The viral titers were estimated with an AdenoX rapid titer assay kit (Clontech).

Isolation and culture of cells. Mouse embryonic stem (ES) cells were isolated from blastocysts obtained from C57BL/6 mice expressing a GFP transgene engineered to be expressed specifically in chondrocytes (*Col2-GFP*), as previously described (29). *Col2-GFP* ES cells were cultured in high-glucose Dulbecco's modified Eagle's medium (DMEM; Sigma, St. Louis, MO) supplemented with β -mercaptoethanol (100 μ M), leukemia inhibitory factor (1,000 units/ml), nonessential amino acids (1%), penicillin (50 units/ml), streptomycin (50 μ g/ml), and fetal bovine serum (FBS; 15%) (JRH Biosciences, Lenexa, KS), as previously described (30). To generate *Col2-GFP* mice, the 6.3-kb *Col2a1* promoter region directing chondrocyte-specific expression was released from the plasmid p3000i3020Col2a1 (a generous gift from Dr. Benoit de Crombrughe, M. D. Anderson Cancer Center, Houston, TX) and subcloned into the pEGFP-1 vector (Clontech). The *Col2-GFP* transgene was then excised and purified for microinjection. Pronuclear injection and subsequent selection of founders were performed as previously described (31).

Human mesenchymal stem cells (MSCs) and adult human dermal fibroblasts (DFs) were purchased from Cambrex (East Rutherford, NJ). Human MSCs were cultured in MSC growth medium at 37°C under 5% CO₂. Adult human DFs were cultured in high-glucose DMEM supplemented with

penicillin (50 units/ml), streptomycin (50 μ g/ml), and FBS (10%).

HuH-7 cells (RCB1366) were obtained from the RIKEN Cell Bank (Tsukuba, Japan). HeLa cells (JCRB9004) were obtained from the JCRB Cell Bank (Osaka, Japan). HEK 293 cells were purchased from Clontech. All cell lines were cultured at 37°C under 5% CO₂ in high-glucose DMEM supplemented with penicillin (50 units/ml), streptomycin (50 μ g/ml), and FBS (10%).

In vitro cartilage formation by Sox gene transfer. Embryoid bodies were formed by 3-dimensional (3-D) suspension culture for 5 days and subsequent 2-D adhesive culture on gelatin-coated plates for 3 days. Then, the embryoid bodies were transduced with adenoviruses expressing the various genes listed above, including the SOX trio at 100 multiplicities of infection (MOI). Chondrogenic differentiation was detected as fluorescence by confocal fluorescent microscopy.

For spheroid culture, human MSCs and adult human DFs were cultured in 100-mm dishes until confluency, and adenoviruses expressing the SOX genes were transduced at 50 MOI. Two days after transduction, cells were trypsinized and 500,000 cells per tube were gently centrifuged to form spheroids. Spheroids were cultured in serum-free high-glucose DMEM or in chondrogenic medium, which consisted of 300 ng/ml of BMP-2 (Yamanouchi, Tokyo, Japan) and 10 ng/ml of TGF β 3 (Techne, Princeton, NJ) in addition to high-glucose DMEM supplemented with 10⁻⁷M dexamethasone, 50 μ g/ml of ascorbate, 40 μ g/ml of proline, 100 μ g/ml of pyruvate, and 1 \times insulin-transferrin-selenium+1 (Sigma). Cells were collected at 3, 7, 14, and 21 days after spheroid formation for histochemical analyses and real-time PCR.

For analysis of monolayer-cultured human MSCs and adult human DFs, SOX genes were transduced at 50 MOI. Cells were collected at 5, 9, 16, and 23 days after transduction for real-time PCR. Three-dimensional culture on collagen gel was performed with 3-D Collagen Cell Culture system (Koken, Tokyo, Japan), according to the manufacturer's instructions. The transduced human MSCs and adult human DFs were trypsinized 2 days after transduction and seeded onto a DMEM-containing collagen gel at a density of 250,000 cells/cm² in 24-well plates and then cultured in serum-free DMEM. Cells were collected at 7, 14, and 21 days of 3-D culture. In each culture system, the medium was replaced every 3–4 days.

Transfections of HuH-7, HeLa, and HEK 293 cell lines with GFP-SOX expression vectors were performed with FuGENE 6 transfection reagent (Roche, Mannheim, Germany). In cotransfection, the same amount of total DNA was used, and all plasmids were added in an equal ratio.

Real-time PCR analysis. Total RNAs from cells were isolated with an RNeasy mini kit (Qiagen, Hilden, Germany), according to the manufacturer's instructions. All total RNA samples were treated with DNase I. Total RNAs (50 ng to 1 μ g) were reverse-transcribed with MultiScribe reverse transcriptase (ABI, Foster City, CA) and random hexamers in a 50- μ l reaction volume, according to the manufacturer's instructions, and 1 μ l of each reverse transcriptase reaction was used as a template for the second-step SYBR Green real-time PCR. The full-length or partial-length cDNA of target genes, including PCR amplicon sequences, were amplified by PCR, cloned into pCR-TOPO Zero II or pCR-TOPO II vectors (Invitrogen, Carlsbad, CA), and used as standard templates

after linearization. QuantiTect SYBR Green PCR Master Mix (Qiagen) was used for the second-step SYBR Green real-time PCR according to the manufacturer's instructions. SYBR Green PCR amplification and real-time fluorescence detection were performed with an ABI 7700 Sequence Detection system. All reactions were run in quadruplicate. Copy numbers of target gene messenger RNA (mRNA) in each total RNA were calculated by reference to standard curves and were adjusted to the human or mouse standard total RNA (ABI) with the human GAPDH or rodent Gapdh as an internal control.

Each primer position in the coding sequences of target genes is described below. SOX5 and SOX6 primer sets were designed on the N-terminal domain of their long isoforms. The human set was as follows: for aggrecan, 6497–6796; for chondromodulin 1, 175–431; for COL2A1, 3856–4123; for COL9A1, 338–635; for COL10A1, 1641–1843; for COL11A2, 2543–2836; for matrilin 3, 232–422; for SOX5, 354–854; for SOX6, 315–593; for SOX9, 651–762; for RUNX2, 1270–1447; for COL1A1, 1184–1411; and for osteopontin (OPN), 251–446.

The mouse set was as follows: for aggrecan, 6013–6177; for chondromodulin 1, 192–474; for Col2a1, 3713–3951; for Col9a1, 1969–2196; for Col11a2, 910–1120; for Sox5, 1775–2010; and for Sox6, 2114–2271.

Western blot analysis. Western blot analysis was performed with cell extracts from SOX-overexpressing cell lines, human MSCs, and adult human DFs. Whole cell lysates or nuclear extracts (5 μ g) were separated by 5–15% sodium dodecyl sulfate-polyacrylamide gel electrophoresis and transferred to polyvinylidene difluoride filters. The filters were incubated with an anti-GFP antibody (1:200; Clontech), anti-SOX antibody mixture (1:200–1:1,000 each; Santa Cruz Biotechnology, Santa Cruz, CA, and a generous gift from Dr. Yoshihiko Yamada, National Institutes of Health, Bethesda, MD, and Dr. Tomoatsu Kimura, Toyama Medical and Pharmaceutical University, Toyama, Japan). Antigen-antibody complexes were detected with horseradish peroxidase-conjugated secondary antibodies and visualized with the use of an ECL-Plus system (Amersham, Piscataway, NJ).

Histologic analysis. Spheroids and mouse tibias were fixed overnight at 4°C in 4% paraformaldehyde/phosphate buffered saline, transferred to 70% ethyl alcohol, and stored at 4°C until they were used. Subsequently, the samples were either frozen in OCT compound and then sectioned at 10 μ m or embedded in paraffin and sectioned at 5 μ m. Sections were stained with Alcian blue, toluidine blue, or Safranin O to evaluate the cartilaginous matrix, and with hematoxylin and eosin to evaluate the morphology, as previously described (32). Immunohistochemistry for Col2 and LacZ was performed as previously described (32).

In vivo SOX gene transfer. Ten 8-week-old C57BL/6J mice were divided into 2 groups and anesthetized with an intraperitoneal injection of pentobarbiturate (5 mg/100 gm of body weight). Then, 10 μ l of a suspension of adenovirus vector expressing LacZ or the SOX trio (10⁸ MOI) was injected into the subcutaneous tissue in front of the anteromedial diaphysis of the tibia. The mice were killed 1 week after surgery, and the entire tibia and surrounding tissue were harvested for histologic and immunohistochemical analyses. Whole tibias were dissected and fixed for 2 hours in 4% paraformaldehyde/phosphate buffered saline, pH 7.4, and decalcified for 2 weeks

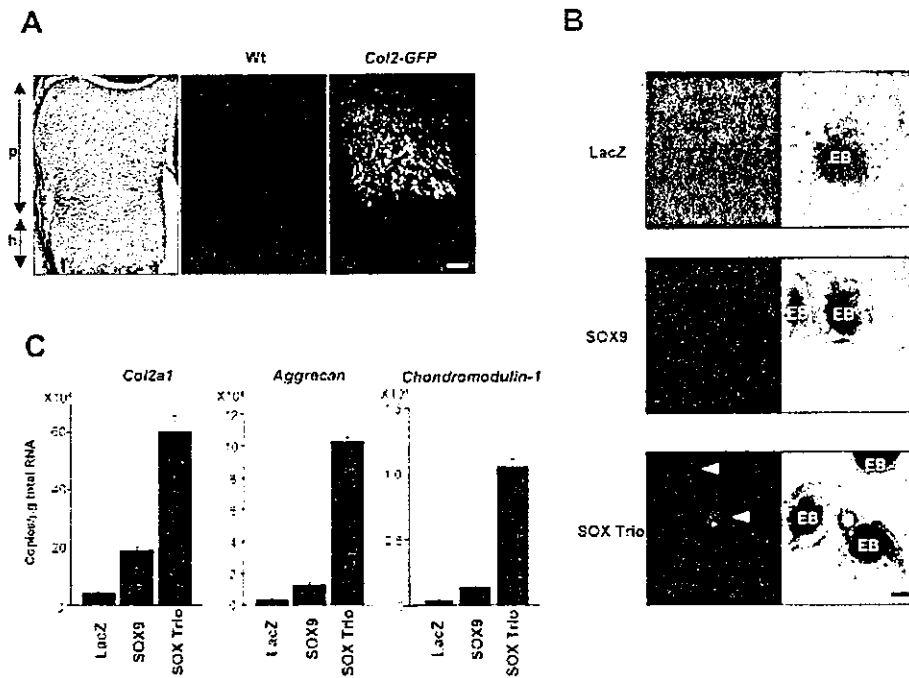


Figure 1. Induction of chondrocytic phenotypes in embryonic stem (ES) cells by the SOX trio. **A**, Fluorescence of growth plate chondrocytes from the *Col2-GFP*-transgenic mouse at embryonic day 18.5. The tibias from wild-type (Wt) and *Col2-GFP* neonate mice were sectioned, and the distal portions were examined by fluorescence microscopy. The morphology of the growth plate is shown at the left with hematoxylin and eosin staining. **p** = proliferating layer of growth plate chondrocytes; **h** = hypertrophic layer of growth plate chondrocytes. Bar = 100 μ m. **B**, Fluorescence of *Col2-GFP* ES cells treated with the combination of SOX5, SOX6, and SOX9 (the SOX trio). LacZ, SOX9, or the SOX trio was adenovirally expressed in embryoid bodies (EB) of ES cells established from the *Col2-GFP*-transgenic mouse, and fluorescence was evaluated on day 3 after transduction (arrowheads). The left half of each panel shows green fluorescence protein (GFP) fluorescence; the right half shows a merging of the GFP fluorescence image and the transmitted image. Bar = 200 μ m. **C**, Expression of the cartilage marker genes *Col2a1*, *Aggrecan*, and *Chondromodulin 1* by ES cells treated with LacZ, SOX9, or the SOX trio for 7 days. Levels of mRNA expression were analyzed by real-time polymerase chain reaction.

in 10% EDTA, pH 7.4. After processing and embedding in paraffin, 3- μ m sagittal sections were cut and stained with Safranin O and fast green. Immunohistochemistry for type II collagen was performed as previously described (32).

Animal care was in accordance with the policies of the University of Tokyo School of Medicine.

GenBank sequences. Human gene sequences were obtained from GenBank (accession nos. M55172 for *AGGREGAN*, AB006000 for *CHONDROMODULIN 1*, X16468 for *COL2A1*, X54412 *COL9A1*, X60382 for *COL10A1*, NM_080679 for *COL11A2*, AJ224741 for *MATRILIN 3*, AB081589 for *SOX5*, AF309034 for *SOX6*, Z46629 for *SOX9*, NM_004348 for *RUNX2*, Z74615 for *COL1A1*, and AF052124 for *OPN*).

Mouse gene sequences were also obtained from GenBank (accession nos. L07049 for *Aggrecan*, NM_010701.1 for *Chondromodulin 1*, NM_031163 for *Col2a1*, D17511 for

Col9a1, NM_009926 for *Coll1a2*, AB006330 for *Sox5*, and U32614 for *Sox6*).

Image acquisition. An Axioskop 2 Plus (Carl Zeiss, Oberkochen, Germany) microscope was used for microscopic observation (bright and fluorescence fields at $\times 100$, $\times 200$, and $\times 400$ magnifications). Photographs were taken with an Axio-Cam HRC (Carl Zeiss) camera, and images were acquired with AxioVision 3.0 software (Carl Zeiss).

RESULTS

Induction of cartilage marker gene expression in ES cells by the SOX trio. To screen for sufficient conditions for chondrogenesis, we needed a monitoring system that could detect chondrocyte differentiation in an easy, precise, and noninvasive manner. For this

purpose, we established transgenic mice expressing the chondrocyte-specific *Col2a1* promoter-*GFP* reporter gene and isolated totipotent, undifferentiated ES cells from them. Since *GFP* expression was specifically localized to the cartilage in these mice (Figure 1A), ES cells from these mice were expected to fluoresce solely upon chondrocyte differentiation. Using this system, we examined the effects of gain and loss of function of representative factors that are known to be important for chondrogenesis: SOX5, SOX6, SOX9, IGF-1, FGF-2, IHH, BMP-2, TGF β , and Wnt proteins.

Since we intended to find factors affecting chondrocyte differentiation directly rather than indirectly, the assessment of fluorescence was done within 3 days after transduction. As a result, no single factor caused fluorescence; hence, we screened for all possible combinations of these factors. It turned out that *GFP* expression was observed only upon treatment with the combination of SOX5, SOX6, and SOX9 (the SOX trio) (Figure 1B), while there was no fluorescence upon treatment with the other combinations, including each SOX alone, within this period (results not shown).

We then examined the expression levels of the cartilage marker genes, which included the cartilaginous collagens (such as *Col2a1*, *Col9a1*, and *Col11a2*), cartilaginous proteoglycans (such as *Aggrecan*), and other cartilage-specific proteins that play key roles in maintaining cartilage structures (such as *Chondromodulin 1*) (33,34). Real-time PCR analysis confirmed that the SOX trio markedly up-regulated the levels of expression of *Col2a1*, *Aggrecan*, and *Chondromodulin 1* compared with SOX9 alone or the LacZ control (Figure 1C).

Induction of chondrocytic phenotypes in human MSCs by the SOX trio. We next examined the effect of the SOX trio on the chondrocyte differentiation of human MSCs. Expression of each SOX protein by adenoviruses was confirmed by Western blot analysis with specific antibodies (Figure 2A). To characterize human MSCs treated with SOX proteins, we evaluated the levels of expression of the cartilage marker genes by real-time PCR (Figure 2B). When cultured with serum-free DMEM in spheroids, human MSCs treated with the LacZ virus did not express detectable levels of the cartilage-specific collagen genes *COL2A1*, *COL9A1*, or *COL11A2* during 3 weeks of spheroid culture. In contrast, when the SOX trio was overexpressed, expression of these genes was detected as early as 3 days after spheroid formation. The number of copies of their mRNA continued to rise during the 3 weeks of spheroid culture. After 3 weeks of spheroid culture, the copy number of *COL2A1* mRNA from human MSCs ex-

ceeded that of *COL2A1* from the tracheal cartilage and articular cartilage.

When an individual SOX gene was transduced, expression of *COL2A1*, *COL9A1*, and *COL11A2* was not detected after 1 week of spheroid culture. After 2 weeks, only human MSCs treated with SOX9 expressed low levels of their mRNA. In contrast, *AGGRECAN* was already expressed at a moderate level even in untreated human MSCs, and its expression was substantially up-regulated by treatment with SOX9 alone or with the SOX trio after 2 weeks of spheroid culture. *CHONDROMODULIN 1* and *MATRILIN 3* were also induced by treatment with the SOX trio. The induction was first observed after 3 days of spheroid culture, and the copy number of their mRNA gradually increased up to 3 weeks.

We then performed histologic examinations of human MSCs treated with LacZ or the SOX trio and cultured in spheroids with serum-free DMEM or the chondrogenic medium containing TGF β and BMP-2 (Figure 2C). Human MSCs treated with the SOX trio and cultured in spheroids with serum-free DMEM produced a proteoglycan-rich extracellular matrix characteristic of cartilage, which showed purple staining (metachromasia) with toluidine blue as early as 1 week after spheroid formation, whereas those treated with an individual SOX failed to show any staining at this stage. After 3 weeks, induction of proteoglycan-rich matrix by the SOX trio became more prominent. At higher magnification, cells in the spheroid were found to be completely surrounded by a proteoglycan-rich matrix, resembling the lacunar structure of cartilage (Figure 2D).

When cultured in the chondrogenic medium, accumulation of proteoglycan-rich matrix was accelerated (Figure 2C). After 1 week, the SOX trio induced abundant matrix production, whereas human MSCs treated with each SOX alone showed only weak production. After 3 weeks, although all spheroids including the LacZ control produced proteoglycan-rich matrix, human MSCs treated with the SOX trio showed the most abundant production. Staining with Alcian blue and Safranin O showed similar results (results not shown).

Production of type II collagen protein was detected by immunohistochemistry (Figure 2E). Human MSCs cultured in spheroids with the chondrogenic medium and treated with the SOX trio produced the most abundant type II collagen protein. Human MSCs cultured with serum-free DMEM and treated with the SOX trio and those cultured in the chondrogenic medium and treated with LacZ produced the second most abundant type II collagen protein. No type II collagen

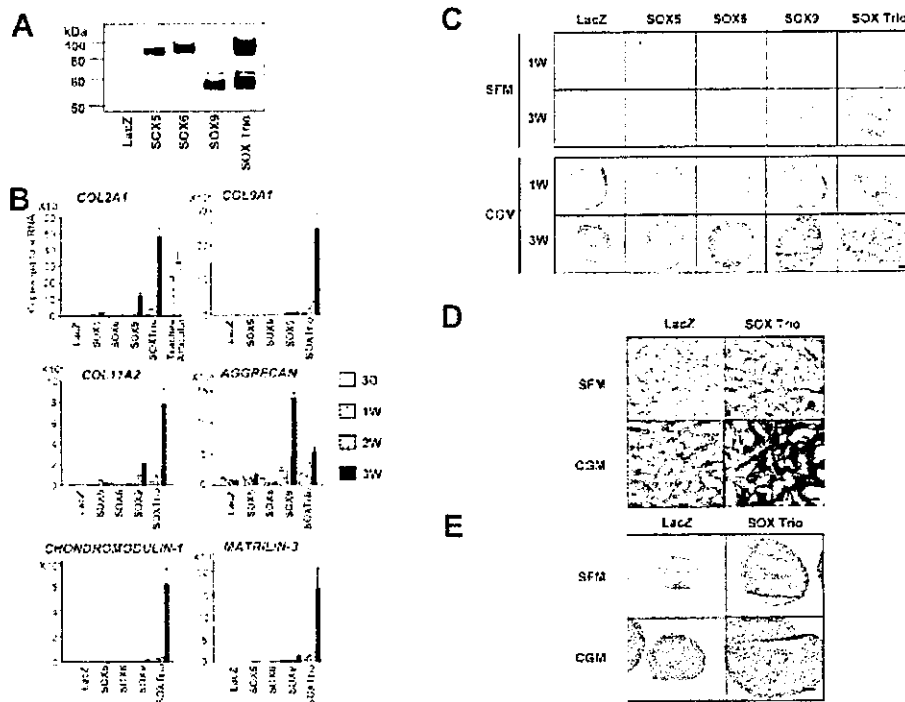


Figure 2. Induction of chondrocytic phenotypes in human mesenchymal stem cells (MSCs) by the SOX trio. **A**, Levels of adenovirally expressed SOX protein expression by human MSCs, as detected by Western blot analysis 5 days after transduction (expected sizes: 82 kd for SOX5, 87 kd for SOX6, and 56 kd for SOX9). **B**, Levels of mRNA expression of the cartilage marker genes *COL2A1*, *COL9A1*, *COL11A2*, *AGGRECAN*, *CHONDROMODULIN 1*, and *MATRILIN 3* by human MSCs. Cells were treated with LacZ, SOX5, SOX6, SOX9, or the SOX trio and cultured in spheroids with serum-free Dulbecco's modified Eagle's medium (DMEM) for 3 days, 1 week, 2 weeks, or 3 weeks, and mRNA expression was analyzed by real-time polymerase chain reaction. As positive controls, *COL2A1* mRNA levels were measured in tracheal and articular cartilage. **C**, Production of proteoglycan-rich matrix by human MSCs treated with LacZ, SOX5, SOX6, SOX9, or the SOX trio and cultured in spheroids with serum-free DMEM (SFM) or chondrogenic medium (CGM) for 1 week or 3 weeks. Spheroid sections were stained with toluidine blue. Proteoglycan-rich matrix stained purple (metachromasia). Bar = 100 μ m. **D**, Higher-magnification views of proteoglycan-rich matrix produced by human MSCs treated with LacZ or the SOX trio and cultured in spheroids with SFM or CGM for 3 weeks. Spheroid sections were stained with toluidine blue. Bar = 20 μ m. **E**, Expression of type II collagen protein by human MSCs treated with LacZ or the SOX trio and cultured in spheroids with SFM or CGM for 3 weeks. Type II collagen protein was detected by immunohistochemistry (brown staining). Bar = 100 μ m.

production was observed in human MSCs cultured in spheroids with serum-free DMEM and treated with LacZ (Figure 2E). Interestingly, the presence of the chondrogenic medium did not cause an increase in mRNA levels of the cartilage marker genes (data not shown).

Induction of chondrocytic phenotypes in non-chondrogenic human immortalized cell lines by the SOX trio. So far, we had found that the SOX trio can induce chondrocytic phenotypes in totipotent ES cells and multipotent MSCs. If the SOX trio constitutes

signals sufficient for the induction of chondrogenesis, it may induce chondrocytic phenotypes in cells already committed to other lineages. To test this possibility, we chose 3 human nonchondrogenic cell lines: HeLa cells derived from the cervix, HuH-7 cells derived from the liver (35), and HEK 293 cells derived from the embryonic kidney (36). Since these cell lines did not tolerate adenoviral transduction well, probably due to rapid proliferation of adenoviruses in these immortalized cells, we used plasmid transfection for gene delivery.

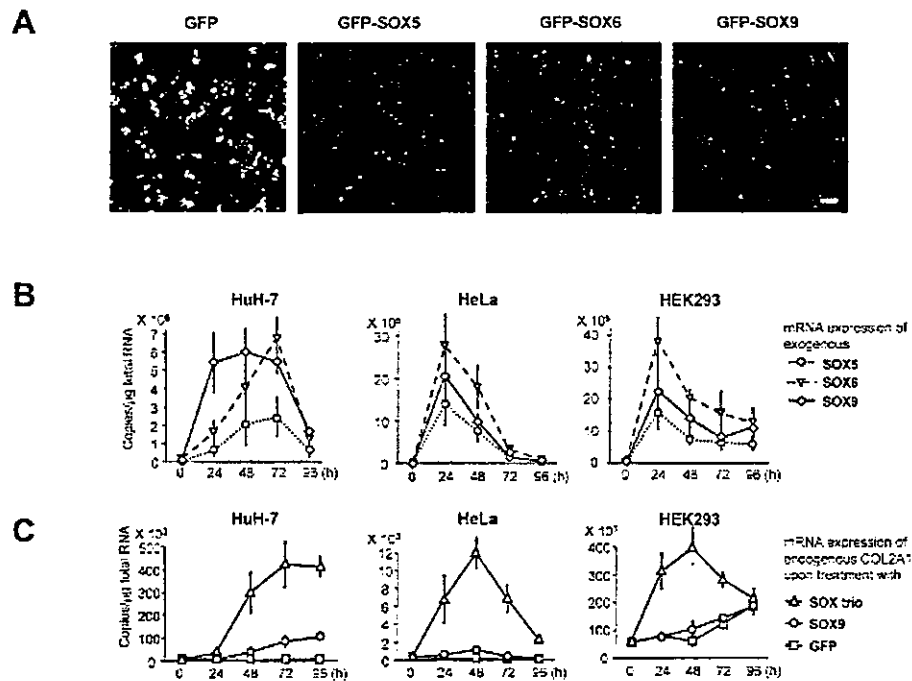


Figure 3. Induction of chondrocytic phenotypes in nonchondrogenic human cell lines by the SOX trio. **A**, Expression of green fluorescence protein (GFP)-tagged SOX proteins in HuH-7 cells. Each of the plasmids expressing GFP-tagged SOX genes was transiently transfected, and their expression levels and subcellular localization were detected as fluorescence using confocal fluorescence microscopy. Bar = 100 μm. **B**, Temporal mRNA expression profiles of exogenous SOX5, SOX6, and SOX9 in HuH-7, HEK 293, and HeLa cells transiently transfected with plasmids expressing these GFP-tagged SOX genes. Cells were cultured in monolayer with Dulbecco's modified Eagle's medium containing 10% fetal bovine serum. Levels of mRNA expression were analyzed by real-time polymerase chain reaction (PCR). **C**, Temporal mRNA expression profiles of endogenous *COL2A1* in HuH-7, HEK 293, and HeLa cells transfected with plasmids expressing GFP, SOX9, or the SOX trio. Levels of mRNA expression were analyzed by real-time PCR.

When each of the plasmids expressing GFP-tagged SOX genes was transiently transfected into these cells, each GFP-tagged SOX protein was well expressed and localized in the nuclei (Figure 3A). Real-time PCR analysis revealed that the peak expression of all SOXs was achieved at 24–72 hours after transfection (Figure 3B). The SOX trio induced *COL2A1* mRNA expression within 3 days (Figure 3C). The temporal profile of *COL2A1* up-regulation correlated well with those of the exogenous SOX genes. Similar results were obtained with *COL9A1* and *COL11A2* (data not shown). It is noteworthy that overexpression of SOX9 alone up-regulated *COL2A1* to some extent in HuH-7 cells expressing moderate levels of endogenous SOX5 and SOX6 (37), but not in HeLa cells expressing no endogenous SOX5 or SOX6.

Induction of chondrocytic phenotypes in adult human DFs by the SOX trio. We further examined whether the SOX trio could induce chondrocytic phenotypes in well-differentiated primary mesenchymal cells such as adult human DFs. Since adult human DFs can be easily harvested and cultured, and grow faster than human MSCs, they could be an alternative cell source for cartilage tissue engineering. Adult human DFs treated with the SOX trio were cultured in spheroids with serum-free DMEM. The SOX trio rapidly induced *COL2A1*, *COL11A2*, *AGGRECAN*, and *MATRILIN 3* within 3 days, and their levels continued to increase for up to 3 weeks (Figure 4A). *COL9A1* and *CHONDROMODULIN 1* were induced at 7 days after spheroid formation, and their expression levels continued to rise for up to 3 weeks as well. Unlike the human MSCs, adult

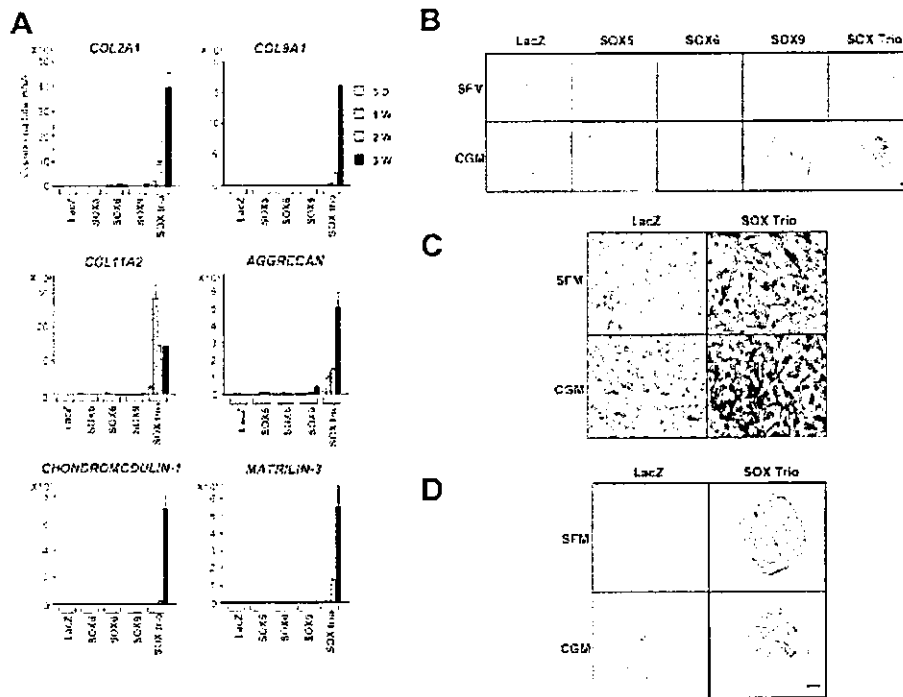


Figure 4. Induction of chondrocytic phenotypes in adult human dermal fibroblasts (DFs) by the SOX trio. **A**, Levels of mRNA expression of the cartilage marker genes *COL2A1*, *COL9A1*, *COL11A2*, *AGGREGAN*, *CHONDROMODULIN 1*, and *MATRILIN 3* by adult human DFs. Cells were treated with LacZ, SOX5, SOX6, SOX9, or the SOX trio and cultured in spheroids with serum-free Dulbecco's modified Eagle's medium (DMEM) for 3 days, 1 week, 2 weeks, or 3 weeks, and mRNA expression was analyzed by real-time polymerase chain reaction. **B**, Production of proteoglycan-rich matrix by adult human DFs treated with LacZ, SOX5, SOX6, SOX9, or the SOX trio and cultured in spheroids with serum-free DMEM (SFM) or chondrogenic medium (CGM) for 3 weeks. Proteoglycan-rich matrix stained purple (metachromasia) with toluidine blue. **C**, Higher-magnification views of proteoglycan-rich matrix produced by adult human DFs treated with LacZ or the SOX trio and cultured in spheroids with serum-free DMEM or chondrogenic medium for 3 weeks. Spheroid sections were stained with toluidine blue. Bar = 20 μ m. **D**, Expression of type II collagen protein by adult human DFs treated with LacZ or the SOX trio and cultured in spheroids with serum-free DMEM or chondrogenic medium for 3 weeks. Type II collagen protein was detected with immunohistochemistry (brown staining). Bar = 100 μ m.

human DFs showed low basal expression of the cartilage marker genes, and treatment with SOX9 alone resulted in very weak or no induction. We compared mRNA expression levels of the cartilage marker genes by adult human DFs and human MSCs that were treated with the SOX trio and cultured in spheroids with serum-free DMEM up to 3 weeks, and found them to be comparable (data not shown).

When cultured in spheroids with serum-free DMEM for 3 weeks, adult human DFs treated with the SOX trio exhibited an accumulation of proteoglycan-rich matrix, whereas those treated with LacZ or with each SOX alone did not (Figure 4B). When cultured with the chondrogenic medium for 3 weeks, adult human

DFs treated with the SOX trio further increased the production of proteoglycan-rich matrix. At higher magnification, cells in the spheroid were found to be surrounded by proteoglycan-rich matrix, resembling the lacunar structure of cartilage (Figure 4C). Adult human DFs treated with SOX9 alone showed weak, focal production of proteoglycan-rich matrix in the presence of the chondrogenic medium, whereas those treated with LacZ, SOX5, or SOX6 did not (Figure 4B). Production of type II collagen protein by adult human DFs treated with the SOX trio and cultured with serum-free DMEM or the chondrogenic medium was confirmed by immunohistochemistry, whereas those treated with LacZ and cultured with serum-free DMEM or the chondrogenic

medium did not exhibit any immunoreactivity (Figure 4D). As with the human MSCs, the presence of the chondrogenic medium did not cause an increase in mRNA levels of the cartilage marker genes (data not shown).

Influence of different culture systems on the induction of chondrocytic phenotypes by the SOX trio. We next examined the effect of different culture systems on chondrocyte differentiation induced by the SOX trio. Three-dimensional cell–cell interactions and the extracellular matrix are known to influence the differentiation potentials of many cell types. Monolayer culture has been reported to be disadvantageous to chondrocyte differentiation, and therefore, spheroid culture and 3-D culture are preferable (38). If the SOX trio provides signals sufficient for chondrogenesis, it may obviate the need for these specific culture formats. To test this possibility, we compared the expression levels of the cartilage marker genes *COL2A1*, *AGGRECAN*, and *CHONDROMODULIN 1* by human MSCs cultured with serum-free DMEM in monolayer, in spheroids, and in 3-D collagen. Even in monolayer culture, treatment with the SOX trio induced high levels of the cartilage marker genes within 1–2 weeks, and their expression levels increased for up to 3 weeks (data not shown). Peak expression levels of the cartilage marker genes in monolayer culture were comparable to those in spheroid culture. Similar results were obtained with adult human DFs (data not shown).

Levels of expression of the cartilage marker genes by human MSCs and adult human DFs treated with the SOX trio and cultured with serum-free DMEM in 3-D collagen cultures were much higher than those cultured in spheroid or monolayer cultures (data not shown), and there was substantial accumulation of proteoglycan-rich matrix secreted into the collagen gel (data not shown).

Induction of the expression of *SOX5* and *SOX6* in vitro by *SOX9*. Conditional ablation of *Sox9* was shown to cause a marked down-regulation of *Sox5* and *Sox6* mRNA expression (19), strongly suggesting that *Sox9* is necessary for the expression of *Sox5* and *Sox6*. In our experiments, ES cells, human MSCs, and adult human DFs treated with *SOX9* alone started to express low levels of some cartilage marker genes after 2 weeks of culture, suggesting the formation of the SOX trio at a later period (Figures 2 and 4). Taken together, it is likely that *SOX9* may induce the expression of *SOX5* and *SOX6*, but the hypothesis has never been directly proven. In our experiment, human MSCs treated with *SOX9* alone and cultured with serum-free DMEM in

3-D collagen for 1 week began to express *SOX5* and *SOX6* mRNA, whereas those treated with *LacZ* and cultured with serum-free DMEM in 3-D collagen did not (Figure 5A). This is the first direct proof that *SOX9* induces *SOX5* and *SOX6*. We also demonstrated that *SOX5* and *SOX6* did not induce each other. Similar results were obtained with ES cells and adult human DFs (data not shown). This induction was also seen in monolayer or spheroid culture, but the degree of up-regulation was smaller and took 2–3 weeks (data not shown).

Suppression of hypertrophic and osteogenic markers by the SOX trio. In human MSCs, mRNA for the gene encoding the type X collagen $\alpha 1$ chain (*COL10A1*), a marker for hypertrophic chondrocytes, was up-regulated when it were cultured in the chondrogenic medium in spheroids (39). Levels of mRNA expression of hypertrophic and osteogenic marker genes, such as *COL10A1*, *RUNX2*, *OPN*, and *COL1A1*, were markedly increased in 3-D collagen culture with serum-free DMEM (Figure 5B). Treatment with *SOX9* alone failed to suppress these genes except for *COL1A1*, whereas treatment with the SOX trio suppressed all of these genes (Figure 5B). In adult human DFs cultured in 3-D collagen with serum-free DMEM, there was no induction of hypertrophic or osteogenic marker genes, regardless of treatment with the SOX trio (data not shown).

In vivo induction of cartilage-like tissue by the SOX trio. To test whether the SOX trio could influence cartilage formation in vivo, we directly introduced the SOX trio genes in the subcutaneous tissue. Adenoviruses expressing the SOX trio were injected into the subcutaneous tissue lying above the tibia, and 1 week after treatment, the mice were killed, and the tissues were harvested and analyzed histologically and immunohistochemically. The viruses transduced subcutaneous cells efficiently, as shown by the positive staining for *LacZ* immunoreactivity (Figure 5C). In all 5 mice treated with the SOX trio, chondrocyte-like cells appeared in the area adjacent to the bone. These cells stained positive for Safranin O and type II collagen immunoreactivity (Figure 5D). In contrast, no such cells were seen in the 5 mice that were treated with *LacZ*.

DISCUSSION

In our screening combinations of factors that are known to be necessary for chondrogenesis, we found that the SOX trio induced chondrocytic phenotypes in totipotent ES cells within 3 days. Previous studies of

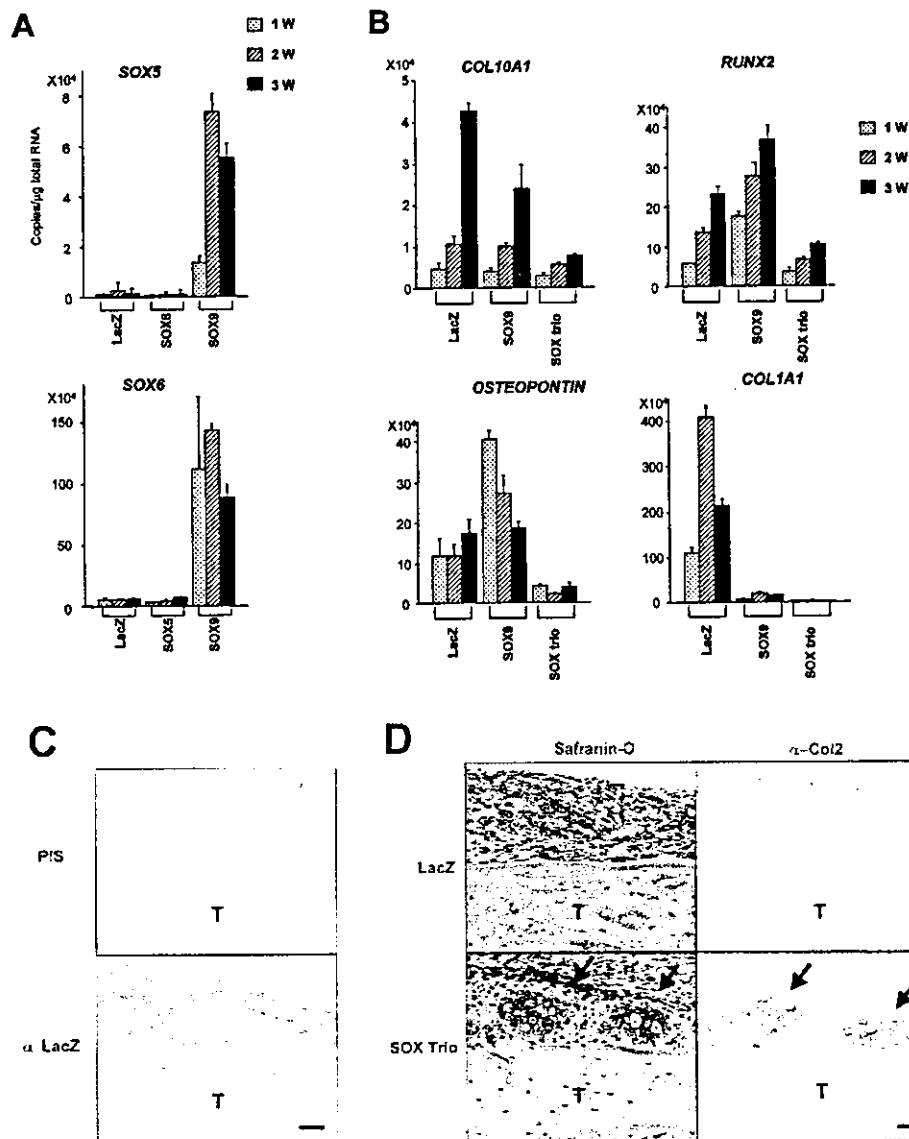


Figure 5. Induction of *Sox5* and *Sox6* expression by SOX9, suppression of hypertrophic and osteogenic differentiation by the SOX trio, and in vivo induction of cartilaginous tissue by the SOX trio. **A**, Levels of mRNA expression of *SOX5* and *SOX6* in human MSCs treated with LacZ, SOX5, SOX6, or SOX9 and cultured in 3-dimensional (3-D) collagen with serum-free Dulbecco's modified Eagle's medium (DMEM) for 1, 2, or 3 weeks, and mRNA expression levels were analyzed by real-time polymerase chain reaction (PCR). **B**, Levels of mRNA expression of the hypertrophic and osteogenic markers *COL10A1*, *RUNX2*, *OSTEOPONTIN*, and *COL1A1* by human MSCs treated with LacZ, SOX9, or the SOX trio and cultured in 3-D collagen with serum-free DMEM for 1, 2, or 3 weeks. Levels of mRNA expression were analyzed by real-time PCR. **C**, Adenoviruses expressing LacZ or the SOX trio were directly injected into the subcutaneous tissue lying above the anteromedial diaphysis of the tibia (T) and the transduction efficiency of adenoviruses was detected by immunohistochemistry for LacZ. Sections were treated with preimmune serum (PIS) or anti-LacZ antibody (α -LacZ). LacZ protein stained brown. Bar = 100 μ m. **D**, Production of proteoglycan-rich matrix and induction of type II collagen protein by the SOX trio. Sections were stained with Safranin O and fast green; cartilage (arrows) stained orange. Type II collagen protein (arrows) was detected by immunohistochemistry (brown staining) with anti-type II collagen antibody (α -Coll2). Bar = 100 μ m.

human MSCs showed that treatment with the chondrogenic supplements TGF β , BMP-2, or both for 2–3 weeks could induce chondrocytic phenotypes (39,40). In the present study, the SOX trio successfully induced chondrocytic phenotypes in human MSCs cultured in serum-free DMEM containing no supplements. Moreover, human MSCs treated with the SOX trio expressed the cartilage marker genes more rapidly and more potently than did those treated with the conventional chondrogenic method, and their levels of mRNA expression induced by the SOX trio were independent of the presence of TGF β and BMP-2. These findings raised the possibility that the SOX trio may provide signals sufficient for the induction of chondrogenesis.

We found that the SOX trio induced cartilage-specific genes that did not belong to collagens or proteoglycans: *MATRILIN 3* and *CHONDROMODULIN 1*. Expression of *MATRILIN 3* is highly specific for cartilage (33). Mutations in *MATRILIN 3* cause a type of human chondrodysplasia known as multiple epiphyseal dysplasia, which is characterized by early-onset heritable osteoarthritis (33). Expression of *CHONDROMODULIN 1* is also specific for cartilage. *CHONDROMODULIN 1* stimulates chondrocyte proteoglycan synthesis and inhibits capillary network formation (34,41). The induction of these genes as well as cartilaginous collagens and proteoglycans by the SOX trio further supports the notion that the SOX trio may provide sufficient signals for the induction of chondrogenesis.

A recent study revealed that in vitro chondrogenesis of murine bone marrow-derived MSCs was enhanced by the overexpression of SOX9 (42). Our data with human MSCs partially support this, in that the cartilage marker genes (*COL2A1*, *COL11A2*, and *AGGRECAN*) were induced in human MSCs treated with SOX9 alone. However, the levels of *COL2A1* and *COL11A2* expression were much lower than those induced in human MSCs treated with the SOX trio. In addition, *COL9A1*, *MATRILIN 3*, and *CHONDROMODULIN 1* were only slightly induced by treatment with SOX9 alone. These findings suggest that SOX9 alone is not sufficient for the induction of chondrogenesis and further emphasizes the importance of the SOX trio.

Although treatment with the SOX trio successfully induced mRNA expression of the cartilage marker genes to a level comparable to that in normal cartilage and induced the production of proteoglycan-rich matrix, the addition of the chondrogenic medium containing TGF β and BMP-2 further increased the accumulation of

proteoglycan-rich matrix without increasing the mRNA expression of the cartilage marker genes in both human MSCs and adult human DFs. Thus, TGF β and BMP-2 may induce other genes that are important for matrix accumulation, or they may be working at the posttranscriptional level. It is noteworthy that in adult human DFs, the chondrogenic medium had no effect on the production of proteoglycan-rich matrix in the absence of treatment with the SOX trio, whereas in human MSCs, the chondrogenic medium had some positive effect in the absence of treatment with the SOX trio. This difference seems to be due to some basal expression of the SOX genes in human MSCs and underscores the important role of the SOX trio in chondrogenesis. The exact mechanism(s) by which TGF β and BMP-2 increase the accumulation of proteoglycan-rich matrix needs to be further investigated and a gene array analysis performed.

Since human MSCs consist of early mesenchymal progenitors that are already committed to some extent, there is a possibility that the SOX trio may merely be expanding the existing chondroprogenitors by increasing their proliferation or suppressing their cell death, rather than directly inducing chondrocytic phenotypes of non-committed cells. To rule out this possibility, the SOX trio was introduced into cell types other than human MSCs. The SOX trio was able to induce chondrocytic phenotypes in ES cells, which are uncommitted and undifferentiated, as well as in cells belonging to other lineages, such as immortalized cell lines derived from the kidney, liver, and cervix. The SOX trio also successfully induced chondrocytic phenotypes in adult human DFs cultured with serum-free DMEM. Expression levels of the cartilage marker genes induced by the SOX trio in adult human DFs were comparable to those in human MSCs induced by the SOX trio and were also independent of treatment with the chondrogenic medium. These findings strongly suggest that expression of the SOX trio is indeed sufficient for the induction of chondrogenesis.

The SOX trio induced chondrocytic phenotypes in cells cultured in monolayer as effectively as in cells in spheroid culture. Since the monolayer culture is usually disadvantageous for in vitro chondrogenesis and since primary chondrocytes cultured in monolayer quickly lose chondrocytic phenotypes through a process known as dedifferentiation, the conventional in vitro chondrogenic methods invariably use spheroid culture or 3-D culture. It is likely that spheroid culture and 3-D culture may provide some unknown signals that are necessary for chondrogenesis but are not present in monolayer culture. The fact that the SOX trio obviated the use of

spheroid culture further supports the importance of the SOX trio in chondrogenesis. At the same time, it shows the limitation of the SOX trio, since the results did not fully match those obtained with the 3-D culture.

We found that the SOX trio helped to maintain the phenotype of permanent cartilage by suppressing the expression of the marker genes for hypertrophic and osteogenic differentiation, which were induced with the conventional chondrogenic method. This finding may reflect in vivo reciprocal expression patterns of the SOX trio and hypertrophic/osteogenic marker genes (21) and enlargement of the hypertrophic zone in the epiphyseal growth plate of *Sox9*^{+/-} mice (43). Although the mechanism of the down-regulation is not yet clear, the SOX trio may directly inhibit hypertrophic and osteogenic markers. Alternatively, proteins such as chondromodulin 1 induced by the SOX trio may down-regulate these markers. In either case, inhibition of hypertrophic and osteogenic markers by the SOX trio is compatible with the notion that the SOX trio directly induces chondrocyte differentiation, and this finding is advantageous for tissue engineering of articular, facial, and tracheal cartilage, which needs to remain nonhypertrophic and nonosteogenic.

This is the first study to show that SOX9 induces *SOX5* and *SOX6*. When treated with SOX9, both human MSCs and adult human DFs began to express *SOX5* and *SOX6* at 1 week after transduction. This finding fits the in vivo sequential expression patterns of *SOX5*, *SOX6*, and *SOX9* and is compatible with the previously reported data (19) that *Sox9*^{flx/flx}, *Prx1-Cre*, and *Col2a1-Cre* mice lost the expression of *Sox5* and *Sox6* in cells that lacked SOX9. This finding is also compatible with our observation that overexpression of SOX9 alone up-regulated cartilage marker genes to some extent in HuH-7 cells expressing moderate levels of endogenous *SOX5* and *SOX6*, but not in HeLa cells expressing no endogenous *SOX5* or *SOX6*. These observations further stress the importance of the SOX trio over individual SOXs in the induction of chondrocytic phenotypes. The mechanism of *SOX5* and *SOX6* induction by SOX9 should be further investigated by analyzing human MSCs and adult human DFs treated with SOX9 alone.

When the SOX trio was adenovirally expressed in the subcutaneous tissue, new cartilage formation was induced. Although the adenoviruses infected most of the cells in the injected area, the strongest induction was observed in the area adjacent to the bone, including the periosteum. This finding suggests that despite the strong chondrogenic actions of the SOX trio, there are cells in the periosteal region that are more susceptible to the

signal. These cells may represent an enrichment of MSCs in the perichondrium.

In conclusion, the findings of the current study strongly suggest that the SOX trio provides signals that are sufficient for the induction of permanent cartilage in vitro. The potent in vitro chondrogenic system of the SOX trio provides a new in vitro model of chondrogenesis, which may help us to better understand the mechanism of chondrogenesis and to advance cartilage regenerative medicine.

ACKNOWLEDGMENTS

We thank Drs. Yoshihiko Yamada and Tomoatsu Kimura for the generous gift of SOX9 antibodies, and Ms Aya Narita, Tomoko Kusadokoro, and Mizue Ikeuchi for technical assistance.

REFERENCES

1. De Crombrughe B, Lefebvre V, Nakashima K. Regulatory mechanisms in the pathways of cartilage and bone formation. *Curr Opin Cell Biol* 2001;13:721-7.
2. Kolettas E, Muir HI, Barrett JC, Hardingham TE. Chondrocyte phenotype and cell survival are regulated by culture conditions and by specific cytokines through the expression of Sox-9 transcription factor. *Rheumatology (Oxford)* 2001;40:1146-56.
3. Stbneur C, Dumontier MF, Guedes C, Fulchignoni-Lataud MD, Tahiri K, Karensty G, et al. Basic fibroblast growth factor as a selective inducer of matrix Gla protein gene expression in proliferative chondrocytes. *Biochem J* 2003;369:63-70.
4. Church VL, Francis-West P. Wnt signalling during limb development. *Int J Dev Biol* 2002;46:927-36.
5. Zehentner BK, Dony C, Burtscher H. The transcription factor Sox9 is involved in BMP-2 signaling. *J Bone Miner Res* 1999;14:1734-41.
6. Tuli R, Tuli S, Nandi S, Wang ML, Alexander FG, Haleem-Smith H, et al. Transforming growth factor- β -mediated chondrogenesis of human mesenchymal progenitor cells involves N-cadherin and mitogen-activated protein kinase and Wnt signaling cross-talk. *J Biol Chem* 2003;278:41227-36.
7. Ng LJ, Wheatley S, Muscat GE, Conway-Campbell J, Bowles J, Wright E, et al. SOX9 binds DNA, activates transcription, and coexpresses with type II collagen during chondrogenesis in the mouse. *Dev Biol* 1997;183:108-21.
8. Zhao Q, Eberspaecher H, Lefebvre V, de Crombrughe B. Parallel expression of Sox9 and Col2a1 in cells undergoing chondrogenesis. *Dev Dyn* 1997;209:377-86.
9. Foster JW, Dominguez-Steglich MA, Guioli S, Kowk G, Weller PA, Stevanovic M, et al. Campomelic dysplasia and autosomal sex reversal caused by mutations in an SRY-related gene. *Nature* 1994;372:525-30.
10. Wagner T, Wirth J, Meyer J, Zabel B, Held M, Zimmer J, et al. Autosomal sex reversal and campomelic dysplasia are caused by mutations in and around the SRY-related gene SOX9. *Cell* 1994;79:1111-20.
11. Bi W, Deng JM, Zhang Z, Behringer RR, de Crombrughe B. Sox9 is required for cartilage formation. *Nat Genet* 1999;22:85-9.
12. Bell DM, Leung KK, Wheatley SC, Ng LJ, Zhou S, Ling KW, et al. SOX9 directly regulates the type-II collagen gene. *Nat Genet* 1997;16:174-8.
13. Bridgewater LC, Lefebvre V, de Crombrughe B. Chondrocyte-

- specific enhancer elements in the Col11a2 gene resemble the Col2a1 tissue-specific enhancer. *J Biol Chem* 1998;273:14998-5006.
14. Lefebvre V, Huang W, Harley VR, Goodfellow PN, de Crombrughe B. SOX9 is a potent activator of the chondrocyte-specific enhancer of the pro α (II) collagen gene. *Mol Cell Biol* 1997;17:2336-46.
 15. Liu Y, Li H, Tanaka K, Tsumaki N, Yamada Y. Identification of an enhancer sequence within the first intron required for cartilage-specific transcription of the α 2(XI) collagen gene. *J Biol Chem* 2000;275:12712-8.
 16. Sekiya I, Tsuji K, Koopman P, Watanabe H, Yamada Y, Shinomiya K, et al. SOX9 enhances aggrecan gene promoter/enhancer activity and is up-regulated by retinoic acid in a cartilage-derived cell line, TC6. *J Biol Chem* 2000;275:10738-44.
 17. Xie WF, Zhang X, Sakano S, Lefebvre V, Sandell LJ. Transactivation of the mouse cartilage-derived retinoic acid-sensitive protein gene by Sox9. *J Bone Miner Res* 1999;14:757-63.
 18. Zhang P, Jimenez SA, Stokes DG. Regulation of human COL9A1 gene expression. Activation of the proximal promoter region by SOX9. *J Biol Chem* 2003;278:117-23.
 19. Akiyama H, Chaboissier MC, Martin JF, Schedl A, de Crombrughe B. The transcription factor Sox9 has essential roles in successive steps of the chondrocyte differentiation pathway and is required for expression of Sox5 and Sox6. *Genes Dev* 2002;16:2813-28.
 20. Smits P, Li P, Mandel J, Deng JM, Behringer RR, de Crombrughe B, et al. The transcription factors L-Sox5 and Sox6 are essential for cartilage formation. *Dev Cell* 2001;1:277-90.
 21. Lefebvre V, Li P, de Crombrughe B. A new long form of Sox5 (L-Sox5), Sox6 and Sox9 are coexpressed in chondrogenesis and cooperatively activate the type II collagen gene. *EMBO J* 1998;17:5718-33.
 22. Miyagishi M, Taira K. RNAi expression vectors in mammalian cells. *Methods Mol Biol* 2004;252:483-91.
 23. Matsumoto M, Ogawa W, Teshigawara K, Inoue H, Miyake K, Sakaue H, et al. Role of the insulin receptor substrate 1 and phosphatidylinositol 3-kinase signaling pathway in insulin-induced expression of sterol regulatory element binding protein 1c and glucokinase genes in rat hepatocytes. *Diabetes* 2002;51:1672-80.
 24. Yamanaka Y, Tanaka H, Koike M, Nishimura R, Seino Y. PTHR1P rescues ATDC5 cells from apoptosis induced by FGF receptor 3 mutation. *J Bone Miner Res* 2003;18:1395-403.
 25. Long F, Zhang XM, Karp S, Yang Y, McMahon AP. Genetic manipulation of hedgehog signaling in the endochondral skeleton reveals a direct role in the regulation of chondrocyte proliferation. *Development* 2001;128:5099-108.
 26. Ruiz i Altaba A. Gli proteins encode context-dependent positive and negative functions: implications for development and disease. *Development* 1999;126:3205-16.
 27. Fujii M, Takeda K, Imamura T, Aoki H, Sampath TK, Enomoto S, et al. Roles of bone morphogenetic protein type I receptors and Smad proteins in osteoblast and chondroblast differentiation. *Mol Biol Cell* 1999;10:3801-13.
 28. Vleminckx K, Kemler R, Hecht A. The C-terminal transactivation domain of β -catenin is necessary and sufficient for signaling by the LEF-1/ β -catenin complex in *Xenopus laevis*. *Mech Dev* 1999;81:65-74.
 29. Chung UI, Lanske B, Lee K, Li E, Kronenberg H. The parathyroid hormone/parathyroid hormone-related peptide receptor coordinates endochondral bone development by directly controlling chondrocyte differentiation. *Proc Natl Acad Sci U S A* 1998;95:13030-5.
 30. Robertson EJ. Embryoid-derived stem cell lines. In: Robertson EJ, editor. *Teratocarcinomas and embryonic stem cells*. 1st ed. Oxford: IRL Press; 1987. p. 71-112.
 31. Rossert J, Eberspaecher H, de Crombrughe B. Separate cis-acting DNA elements of the mouse pro- α 1(I) collagen promoter direct expression of reporter genes to different type I collagen-producing cells in transgenic mice. *J Cell Biol* 1995;129:1421-32.
 32. Hoshi K, Komori T, Ozawa H. Morphological characterization of skeletal cells in Cbfa1-deficient mice. *Bone* 1999;25:639-51.
 33. Chapman KL, Mortier GR, Chapman K, Loughlin J, Grant ME, Briggs MD. Mutations in the region encoding the von Willebrand factor A domain of matrilin-3 are associated with multiple epiphyseal dysplasia. *Nat Genet* 2001;28:393-6.
 34. Shukunami C, Hiraki Y. Expression of cartilage-specific functional matrix chondromodulin-I mRNA in rabbit growth plate chondrocytes and its responsiveness to growth stimuli in vitro. *Biochem Biophys Res Commun* 1998;249:885-90.
 35. Nakabayashi H, Taketa K, Miyano K, Yamane T, Sato J. Growth of human hepatoma cells lines with differentiated functions in chemically defined medium. *Cancer Res* 1982;42:3858-63.
 36. Graham FL, Smiley J, Russell WC, Nairn R. Characteristics of a human cell line transformed by DNA from human adenovirus type 5. *J Gen Virol* 1977;36:59-74.
 37. Ikeda T, Zhang J, Chano T, Mabuchi A, Fukuda A, Kawaguchi H, et al. Identification and characterization of the human long form of Sox5 (L-SOX5) gene. *Gene* 2002;298:59-68.
 38. Benya PD, Shaffer JD. Dedifferentiated chondrocytes reexpress the differentiated collagen phenotype when cultured in agarose gels. *Cell* 1982;30:215-24.
 39. Sekiya I, Vuoristo JT, Larson BL, Prockop DJ. In vitro cartilage formation by adult human stem cells from bone marrow stroma defines the sequence of cellular and molecular events during chondrogenesis. *Proc Natl Acad Sci U S A* 2002;99:4397-402.
 40. Pittenger MF, Mackay AM, Beck SC, Jaiswal RK, Douglas R, Mosca JD, et al. Multilineage potential of adult human mesenchymal stem cells. *Science* 1999;284:143-7.
 41. Hiraki Y, Mitsui K, Endo N, Takahashi K, Hayami T, Inoue H, et al. Molecular cloning of human chondromodulin-I, a cartilage-derived growth modulating factor, and its expression in Chinese hamster ovary cells. *Eur J Biochem* 1999;260:869-78.
 42. Tsuchiya H, Kitoh H, Sugiura F, Ishiguro N. Chondrogenesis enhanced by overexpression of sox9 gene in mouse bone marrow-derived mesenchymal stem cells. *Biochem Biophys Res Commun* 2003;301:338-43.
 43. Bi W, Huang W, Whitworth DJ, Deng JM, Zhang Z, Behringer RR, et al. Haploinsufficiency of Sox9 results in defective cartilage primordia and premature skeletal mineralization. *Proc Natl Acad Sci U S A* 2001;98:6698-703.

Cyclic GMP-dependent protein kinase II is a molecular switch from proliferation to hypertrophic differentiation of chondrocytes

Hiroataka Chikuda,¹ Fumitaka Kugimiya,¹ Kazuto Hoshi,¹ Toshiyuki Ikeda,¹ Toru Ogasawara,¹ Takashi Shimoaka,¹ Hiroataka Kawano,¹ Satoru Kamekura,¹ Atsuko Tsuchida,² Norihide Yokoi,² Kozo Nakamura,¹ Kajuro Komeda,² Ung-il Chung,¹ and Hiroshi Kawaguchi^{1,3}

¹Department of Sensory and Motor System Medicine, Faculty of Medicine, University of Tokyo, Bunkyo, Tokyo 113-8655, Japan; ²Division of Laboratory Animal Science, Animal Research Center, Tokyo Medical University, Shinjuku, Tokyo 160-8402, Japan

The Komeda miniature rat Ishikawa (KMI) is a naturally occurring mutant caused by an autosomal recessive mutation *mri*, which exhibits longitudinal growth retardation. Here we identified the *mri* mutation as a deletion in the rat gene encoding cGMP-dependent protein kinase type II (cGKII). KMIs showed an expanded growth plate and impaired bone healing with abnormal accumulation of postmitotic but nonhypertrophic chondrocytes. Ex vivo culture of KMI chondrocytes reproduced the differentiation impairment, which was restored by introducing the adenovirus-mediated *cGKII* gene. The expression of *Sox9*, an inhibitory regulator of hypertrophic differentiation, persisted in the nuclei of postmitotic chondrocytes of the KMI growth plate. Transfection experiments in culture systems revealed that cGKII attenuated the *Sox9* functions to induce the chondrogenic differentiation and to inhibit the hypertrophic differentiation of chondrocytes. This attenuation of *Sox9* was due to the cGKII inhibition of nuclear entry of *Sox9*. The impaired differentiation of cultured KMI chondrocytes was restored by the silencing of *Sox9* through RNA interference. Hence, the present study for the first time shed light on a novel role of cGKII as a molecular switch, coupling the cessation of proliferation and the start of hypertrophic differentiation of chondrocytes through attenuation of *Sox9* function.

[*Keywords*: KMI; cGKII; *Sox9*; chondrocyte; hypertrophy; endochondral ossification]

Received May 20, 2004; revised version accepted August 4, 2004.

Skeletal growth is determined mainly by the process of endochondral ossification in the cartilaginous growth plate, which consists of the resting, proliferative, and hypertrophic zones of chondrocytes, typically in orderly columnar arrays. In this process, chondrocytes that arise from mesenchymal cells undergo proliferation, terminal differentiation into hypertrophic cells, and synthesis of the cartilage matrix, which finally calcifies and is replaced by bone (Kronenberg 2003). The start of hypertrophic differentiation occurs concurrently with the cessation of chondrocyte proliferation. To date, several molecular signalings have been implicated in the switching between proliferation and terminal differentiation in other cell types (Sorrentino et al. 1990; Umek et al. 1991; Tao and Umek 2000); however, the molecular mechanism that couples the cessation of proliferation and the

start of hypertrophic differentiation of chondrocytes remains an enigma.

The Komeda miniature rat Ishikawa (KMI), which was discovered in a closed colony of Wistar rats and was established as a segregating inbred, is a naturally occurring dwarf mutant caused by an autosomal recessive mutation *mri* (Serizawa 1993). Homozygous mutants (*mri/mri*) were born and grew normally until 3–4 wk of age, when they gradually started to develop longitudinal growth retardation without other organ abnormalities. In the present study we identified the *mri* mutation as a deletion in the rat gene encoding cGMP-dependent protein kinase type II (cGKII) by a positional candidate cloning strategy. cGKII is a membrane-bound kinase which is activated by intracellular cGMP, and is known to be expressed abundantly in the intestinal mucosa, kidney, lung, brain, and cartilage (Ruth 1999; Hofmann et al. 2000). This study further investigated the cellular and molecular mechanisms underlying the impairment of endochondral ossification by the cGKII deficiency.

³Corresponding author.
E-MAIL kawaguchi-ort@h.u-tokyo.ac.jp; FAX 81-3-3818-4082.
Article and publication are at <http://www.genesdev.org/cgi/doi/10.1101/gad.1224204>.

Results

Longitudinal growth retardation in KMI (*mri/mri*)

KMIs developed dwarfism with short limbs and trunk compared to the wild-type littermates (Fig. 1A). Growth curves indicated that KMIs started to show the axial growth retardation postnatally at 4 wk of age, although there was no difference between wild-type and heterozygote (*+mri*) rats in either sex, confirming an autosomal recessive inheritance (Fig. 1B). The trunk of the KMIs was about 30% shorter than those of wild-type and *+mri* littermates at 10 wk of age. Skeletal X-ray analysis at this age revealed no appreciable changes between wild type and KMI in the width of calvarium, which is formed through intramembranous ossification; however, the longitudinal lengths of femora, tibiae, and vertebrae, all of which are formed through endochondral ossification, were 20%–30% shorter in KMI than in wild type (Fig. 1C,D). In the long bones of KMI, the height of the epiphyseal growth plate was greater than that in wild type, indicating that the growth retardation in KMI resulted from the impairment of endochondral ossification in the growth plate.

Positional cloning of the *mri* mutation

We first genotyped simple sequence length polymorphism (SSLP) markers throughout the rat genome on the

backcross progeny and detected putative linkage at the *D14Rat6* marker on rat chromosome 14. Further genetic mapping localized the *mri* locus to a 1.2-cM interval on rat chromosome 14 flanked by markers *D14Rat5* and *D14Rat80*. Comparative mapping analysis revealed that the region was orthologous to the regions on mouse chromosome 5 and human chromosome 4, in which several candidate genes including *Bmp3* and *cGKII* (also known as *Prkg2*) were identified (Fig. 2A). Although the *Bmp3* gene encoding a bone morphogenetic protein (BMP) first drew our attention, our studies revealed this gene unlikely to be causative of the KMI phenotype. The expression of the *Bmp3* gene was not different between wild type and KMI, and the sequencing analysis showed only a few silent variants (data not shown). Furthermore, the *Bmp3* null mice are reported to exhibit normal body size but increased bone density [Daluiski et al. 2001], which is different from the KMI phenotypes.

We then performed an RT-PCR analysis of the *cGKII* gene, and found that the *cGKII* transcript from the brain of the KMI mutant was shorter than that from wild type (Fig. 2B). Sequencing analysis disclosed that exon 3 of the *cGKII* gene was directly spliced onto exon 6 (Fig. 2C). This 220-bp deletion spanning exons 4 and 5 resulted in a frame shift and a premature stop codon, predicting a truncated product that lacks the entire kinase domain (Fig. 2D). We further carried out inter-exon PCR between exons 3 and 6 of the genomic DNA, and found an ~5-kb

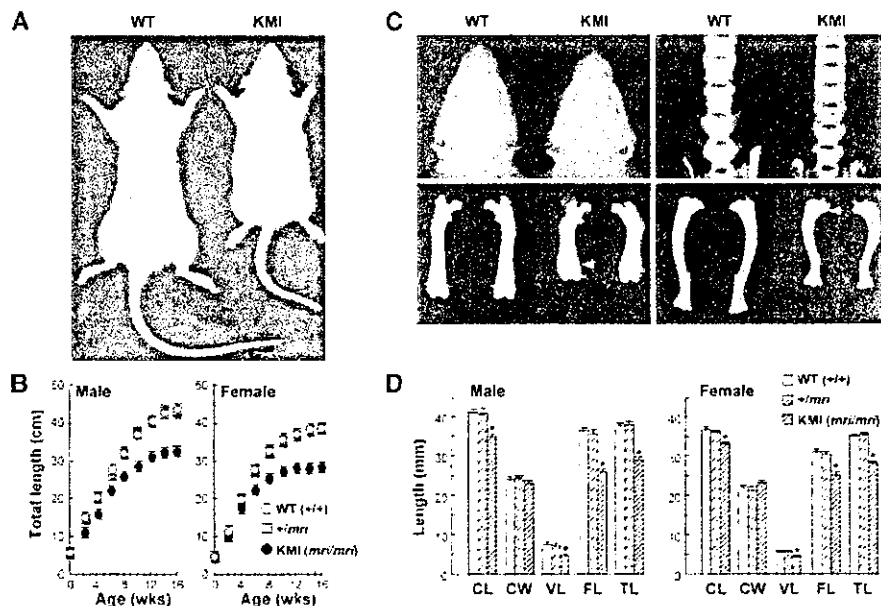


Figure 1. Longitudinal growth retardation in KMI (*mri/mri*). (A) Gross appearance of wild-type (WT) and KMI littermates at 10 wk of age. (B) Growth curves of wild-type (WT; *+/+*), heterozygote (*+mri*), and homozygote (KMI, *mri/mri*) rats determined by the total axial length (from nose to tail end). The symbols of *+mri* are behind those of wild-type rats. Data are expressed as means (symbols) \pm S.E.M. (error bars) for 12 rats/group. (C) Plain X-ray images of wild-type (WT) and KMI littermates at 10 wk. Arrowheads indicate the expanded growth plates in KMI. (D) Bone lengths of wild type (WT), *+mri*, and KMI at 10 wk. (CL) Naso-occipital length of the calvarium; (CW) maximal interparietal distance of the calvarium; (VL) fifth lumbar vertebral length; (FL) femoral length; (TL) tibial length. Data are means (bars) \pm S.E.M. (error bars) for 12 rats/group. [*] $P < 0.05$ vs. wild type.

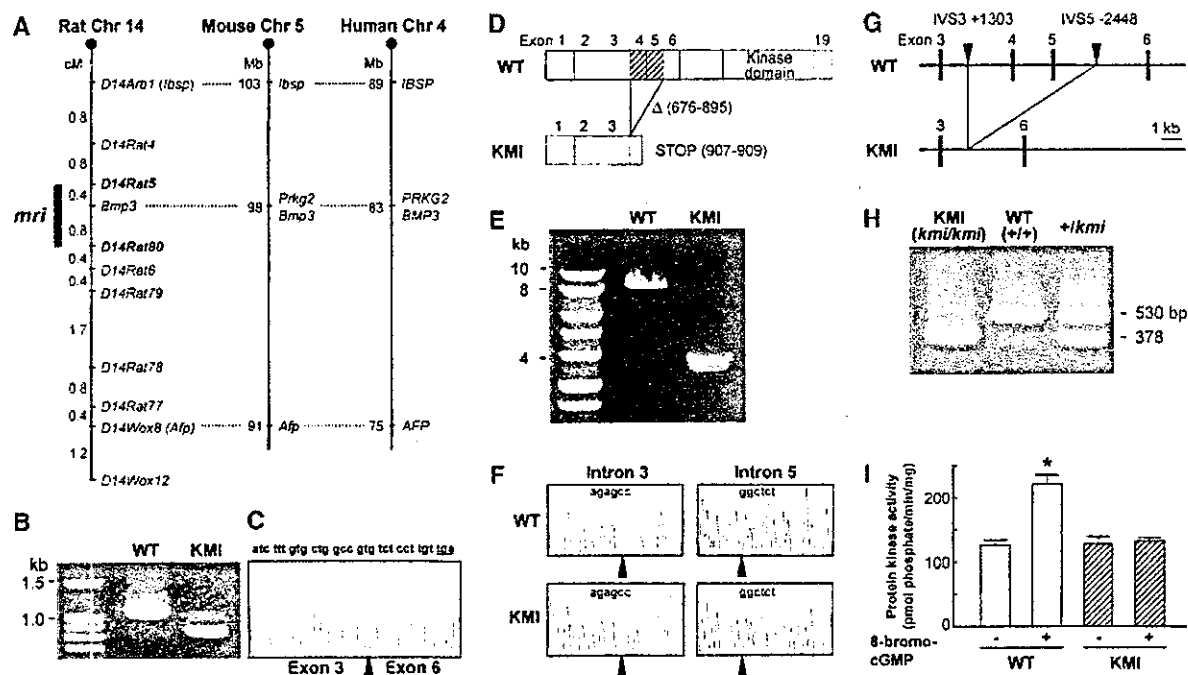


Figure 2. Identification of the *mri* mutation. [A] Comparative mapping of the *mri* region in the rat, mouse, and human chromosomes. The *mri* locus, which was mapped to a 1.2-cM interval between markers *D14rat5* and *D14rat80*, is shown as a bold line. [B] RT-PCR products of the rat cGKII from the brains of wild-type (WT) and KMI littermates. [C] Sequence analysis of transcript of the *cGKII* gene from the KMI mutant. Exon 3 is directly spliced onto exon 6, with the boundary indicated by the arrowhead. The frame shift causes amino acid substitutions and a premature stop codon. [D] Schematic representation of the prematurely truncated cGKII protein in the KMI mutant. Nucleotide sequence analyses of the cDNA identified a 220-bp deletion (676–895) corresponding to exons 4 and 5. [E] Interexon PCR between exons 3 and 6 using the genomic DNA from wild type (WT) and KMI indicated an ~5-kb deletion in the KMI. [F] Sequence analyses of genomic DNA of wild type (WT) and KMI identified breakpoints in introns 3 and 5 (arrowheads). A common sequence, "AGAGCC", was found at the two breakpoints. [G] Schematic representation of the *mri* mutation as an ~5-kb deletion in the *cGKII* gene. Sequence analyses disclosed the deletion from IVS3+1303 to IVS5–2448 in KMI. [H] Genotyping of KMI (*mri/mri*), wild-type (WT; +/+), and +/*mri* rats. A longer amplicon (530 bp) was amplified from wild-type allele, and a shorter amplicon (378 bp) from the mutated allele. [I] Lack of cGMP-dependent protein kinase activity of the KMI brain extract determined by the *in vitro* kinase assay in the presence and absence of 8-bromo-cGMP. Data are means (bars) \pm S.E.M. (error bars) of six samples/group. (*) $P < 0.01$, significant effect of 8-bromo-cGMP.

deletion in the *cGKII* gene of KMI (Fig. 2E). Sequencing analysis identified the breakpoints in introns 3 and 5, both of which had a common sequence, "AGAGCC" (Fig. 2F), creating a deletion from intervening sequence (IVS)3+1303 to IVS5–2448 (Fig. 2G). To confirm that this deletion in the *cGKII* gene was responsible for the KMI phenotype, we designed PCR primers to detect this genomic deletion, and found complete cosegregation of the genotypes KMI (*mri/mri*), wild type (+/+), and +/*mri* with the phenotypes (Fig. 2H). To test whether the *mri* mutation in the *cGKII* gene resulted in loss of its function, tissue extract from brain that is known to express high levels of cGKII was assayed for the kinase activity. The *in vitro* kinase assay revealed that the wild-type extract showed a significant increase in the kinase activity by the stimulation with the cGMP analog 8-bromo-cGMP; however, the increase was not observed in the KMI extract (Fig. 2I). Taken together, these results strongly suggested that the deletion in the *cGKII* gene resulted in loss of its function and caused dwarfism in KMI.

Abnormal endochondral ossification in the growth plate and the fracture callus of KMI

We first investigated the expression pattern of cGKII in the proximal growth plates of the wild-type and KMI tibiae at 10 wk of age. Immunohistochemical analysis of the wild-type growth plate revealed that cGKII was expressed predominantly in the late proliferative and prehypertrophic chondrocytes, preceding the start of hypertrophic differentiation; however, no immunoreactivity for cGKII was observed in the KMI growth plate (Fig. 3A, α -cGKII).

To elucidate the cellular mechanisms underlying the dwarfism due to the cGKII dysfunction in KMI, we performed histological analyses of the growth plates. At birth, growth plates showed no discernible difference between wild type and KMI (Fig. 3A, HE, E18.5). Pathological changes gradually became evident postnatally after 4–5 wk of age, and at 10 wk the height of the KMI growth plate was about 2.5-fold greater than that of wild type

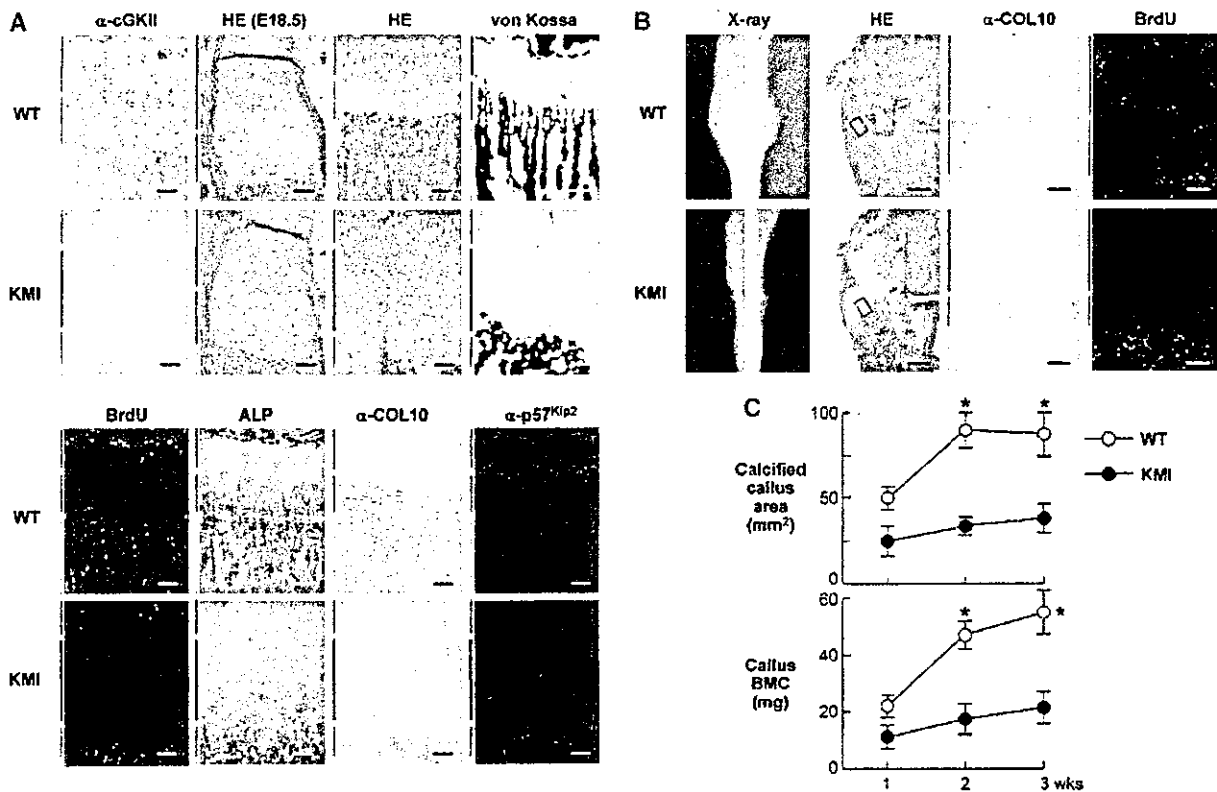


Figure 3. Comparison of endochondral ossification in the growth plate (A) and the bone fracture callus (B,C) between wild type (WT) and KMI. Blue, red, and green bars indicate layers of proliferative zone, hypertrophic (including prehypertrophic) zone, and primary spongiosa, respectively. Black bar indicates the abnormal intermediate zone that is seen only in KMI. (A) Histological findings of the proximal growth plates in wild-type (WT) and KMI tibiae at 10 wk of age unless otherwise described. (Upper panel) Immunohistochemical staining with an anti-cGKII antibody (α -cGKII), hematoxylin-eosin staining of the humeral growth plates of fetal rats (HE, E18.5), HE staining (HE), and von Kossa staining (von Kossa). (Lower panel) BrdU labeling (BrdU), alkaline phosphatase staining (ALP), immunohistochemical stainings with anti-type X collagen (α -COL10), and anti-p57^{Kip2} (α -p57^{Kip2}) antibodies. Bars, 50 μ m. (B) Radiological and histological findings of the fracture callus 2 wk after the surgery. After exposing the right tibiae of 10-week-old rats, a transverse osteotomy was performed at the midshaft with a bone saw and was stabilized with an intramedullary nail. Plain X-ray images (X-ray), HE staining (HE; inset boxes indicate the regions of the right two figures), immunohistochemical staining with an anti-type X collagen antibody (α -COL10), and BrdU labeling (BrdU). Bars: HE, 500 μ m; right two figures, 50 μ m. (C) Time course of the calcified area and the bone mineral content (BMC) of the callus at the fracture site measured by a single energy X-ray absorptiometry. Data are mean (symbols) \pm S.E.M. (error bars) of eight rats/genotype. (*) $P < 0.01$ vs. wild type.

($665 \pm 47 \mu\text{m}$ vs. $255 \pm 34 \mu\text{m}$, mean \pm S.E.M., $n = 8$, respectively), although the columnar structure was relatively preserved (Fig. 3A, HE). This increase was due to an intermediate layer of accumulated abnormal chondrocytes in the KMI growth plate (Fig. 3A, HE, black bar). Although the cell size of chondrocytes in the KMI hypertrophic zone seemed somewhat smaller than that in wild type, matrix mineralization determined by von Kossa staining appeared normal in KMI (Fig. 3A, von Kossa).

To further characterize the abnormal chondrocytes in the intermediate layer of the KMI growth plate, we examined cellular proliferation by the uptake of BrdU. In wild type, chondrocytes in the proliferating zone and bone marrow cells in the primary spongiosa were actively proliferating as detected by the BrdU uptake (Fig. 3A, BrdU). In KMI, the number of BrdU-positive cells

was slightly decreased in the proliferating zone, and more importantly, no uptake was observed in the intermediate layer, suggesting that these abnormal chondrocytes were postmitotic. We next examined the distributions of alkaline phosphatase (ALP) and type X collagen (COL10) as markers of prehypertrophic and hypertrophic chondrocytes, respectively. Histochemical analyses of the wild-type growth plate revealed that these markers were expressed immediately after the BrdU uptake had disappeared, confirming the coupling of the cessation of proliferation and the start of hypertrophic differentiation (Fig. 3A, ALP and α -COL10). In the KMI growth plate, however, the intermediate layer was stained by neither of the markers, indicating that these abnormal chondrocytes had not started hypertrophic differentiation. In addition, expression of p57^{Kip2}, a key regulator of cell-cycle arrest and differentiation of chondrocytes (Yan et al.